

Original Article

Polycyclic aromatic hydrocarbons (PAHS) accumulation and histopathological biomarkers in gills and mantle of *Lanistes carinatus* (Molluscs, Ampullariidae) to assess crude oil toxicity

Gamatat Osman¹, Mansour Galal¹, Abbas Abul-Ezz², Ahmad Mohammed¹, Mohammed Abul-Ela³ and Asmaa Mostafa Hegazy^{2*}

¹Department of Zoology, Faculty of Sciences, El-Menofeya University, Egypt

²Department of Aquatic Pathology, National Institute of Oceanography and Fisheries (NIOF), Cairo, Egypt

³Chromatographic Laboratory, Analysis and Evaluation Department, Egyptian Petroleum Research Institute (EPRI), Nasr City, Cairo, Egypt

(Article history: Received: March 29, 2017; Revised: June 10, 2017)

Abstract

The freshwater snail *Lanistes carinatus* was tested as bioindicator to assess water quality and identify exposure to oil contaminants. *L. carinatus* was chronically exposed to crude oil at intervals of 24 hours, 15 days and 30 days. The LC₅₀ of crude oil for *L. carinatus* was 700 ppm. HPLC analysis of 16 polycyclic aromatic hydrocarbons (PAHs) in the flesh demonstrated that PAHs accumulation in the treated snails was fluctuated with time. The accumulation is due to their biotransformation process during metabolism. The histopathological observations of the gills and mantle of *L. carinatus* showed pronounced alterations at 24 hours and proliferated at the day 15 but showed a further decline at the day 30 of exposure. These findings seem to be time related and were classified as reversible and irreversible changes. Accordingly, it can be concluded that *L. carinatus* is a typical bioindicator for crude oil pollution.

Key Words: Crude oil, Toxicity, Histopathology, Gill, Mantle, Bioaccumulation, PAHs.

To cite this article: OSMAN, G., GALAL, M., ABDUL-EZZ, A., MOHAMMAD, A., ABUL-ELA., M., HEGAZY, A.M., 2017. Polycyclic aromatic hydrocarbons (PAHS) accumulation and histopathological biomarkers in gills and mantle of *Lanistes carinatus* (Molluscs, Ampullariidae) to assess crude oil toxicity. *Punjab Univ. J. Zool.*, **32**(1): 39-50.

INTRODUCTION

Biomarkers offers an integrated measure on effects of pollutant exposure in wildlife and have been strongly recommended to be included in environmental monitoring programs (Jemec *et al.*, 2010 and Bejarano and Michel, 2016). Snails were also successfully included in *in vitro* experimental designs for inducing and evaluating biomarkers of pollutants (Grosell and Brix, 2009; Osterauer *et al.*, 2009; Tania *et al.*, 2011; Sandrini-Neto *et al.*, 2016) as well as *in vivo* researches (Sarkara *et al.*, 2008, 2014; Sanni *et al.*, 2016).

Crude oil is a typical complex mixture of compounds in which hydrocarbons constitute the majority of these compounds such as polycyclic aromatic hydrocarbons (PAHs). Uptake of these materials was reported in aquatic invertebrates from the ambient environment or accidentally via feeding from contaminated areas (Baker *et al.*, 2012;

Bejarano and Michel, 2016). PAHs are highly lipid-soluble and thus readily absorbed from the gastrointestinal tract of the animals and are rapidly distributed in a wide variety of tissues with a marked tendency for accumulation in liver or lipids.

Metabolism of PAHs in aquatic animals occurs via the cytochrome P450 pathway leading to a phenomenon known as oxidative stress (Jemec *et al.*, 2010; Lushchak, 2011; Liu *et al.*, 2014; Dalzochio *et al.*, 2016). Contaminants-stimulate production of reactive oxygen species (ROS) and the resulting oxidative damage may be a mechanism of toxicity in aquatic organisms exposed to a variety of pollutants (Jemec *et al.*, 2010; Lushchak, 2011; Liu *et al.*, 2014; Cai *et al.*, 2016). Recorded essays of antioxidant defensive responses in some invertebrates due to aromatic hydrocarbons exposure or heavy metals were conducted (Liu *et al.*, 2014; Cai *et al.*, 2016; Sandrini-Neto *et al.*, 2016). Liu *et al.*

(2014) believed that pollutants transfer into diol epoxides resulting from metabolism by the oxidative process causing damage, or moreover, react with DNA producing the essential carcinogenic factor (Sarkara *et al.*, 2014). Gills are multifunctional organs responsible for respiration, osmoregulation, acid base balance and nitrogenous waste excretion. These organs are sensitive to wide variety of chemicals in water. Thus, chronic exposure of snails to pollutants in water and sediments may ultimately impair their respiratory ability. A variety of biomarkers in gill and mantle reflect changes in the concentration and duration of exposure to various pollutants were recorded (Chakraborty *et al.*, 2010; Sawasdee *et al.*, 2011; Andleeb, 2014; Liu *et al.*, 2014; Dalzochio *et al.*, 2016). Dalzochio *et al.* (2016) in their review stated that the analysis of gills of fish and bivalves has been widely used because changes in this organ may lead to the impairment of several functions, including gas exchange, ion regulation and excretion of metabolites. Chakraborty *et al.* (2010) investigated histopathological damages of the gill of *Lamellidens marginalis* leading to its dysfunction for molluscs exposed to sublethal concentrations of sodium arsenite for a maximum period of 30 days.

The United Nations Environment Programme (UNEP) and World Health organization (WHO, 1993) recommended the use of certain biomarkers to assess the impact of pollution. Au (2004) critically reviewed 14 histocytopathological biomarkers. Dalzochio *et al.* (2016) reviewed histopathological biomarkers used to assess the health of aquatic ecosystems in Brazil. This research is aimed to assess *L. carinatus* bioindicator through studying the capacity of the snail to accumulate PAHs at different intervals and investigating the toxicity of crude oil to gill and mantle to reveal the extent of damage leaching to these tissues.

MATERIALS AND METHODS

Experimental animal and maintenance

The experimental studies were carried out on the freshwater snail *Lanistes carinatus* (Oliver, 1804) (Mollusca, Ampullariidae). Laboratory studies were applied on the average size 18-20 mm diameter to be ensured that snails are neither young nor senile. Active and healthy specimens were manually collected by fishermen from River Nile and transferred to the laboratory, where they were shaded for

cercariae parasitism and acclimated to the laboratory conditions for period of 2 weeks in glass aerated stock aquaria. During the acclimation period, snails were fed with lettuce and the water was renewed twice weekly. Two days prior to application of petroleum, snails were transferred from the stock aquaria to the experimental aquaria.

Toxic material used: Crude petroleum oil of Qarun well, Feiyom, Egypt. Density= 0.8127 at 25°C.

Experimental Methods and Design

Toxicity test for crude oil to *L. carinatus* (Litchfield and Wilcoxon, 1949)

This was carried out on 110 snails which were grouped in 11 groups of 10 snails, put in 5L aerated aquaria. A series consisted of 10 crude oil concentrations that would permit the computation of LC₅₀ value were applied on 10 groups of the snails for 96 hrs. The remaining 10 snails were kept as a control. Aquaria were kept covered during the test period and the snails were observed for mortalities and any gross alterations. They were considered dead when they ceased pulling their tentacles when touched with a needle.

Long term exposure experiment

About 100 *L. carinatus* were exposed to sublethal concentrations of 1/10 LC₅₀ in triplets for a period of 30 days. A similar 100 *L. carinatus* were remained as control. In the two groups, the experimental conditions were justified to be identical to those exhibited for the toxicity test. Snails were sampled at periods of 0 hr, 24 hrs, 15 days and 30 days.

Estimation of PAHs burden in experimented snails

At each interval, 40 g of the snail flesh (after removing of the shell and the operculum) were washed in saline and stored at -20°C till processing for HPLC analysis.

Extraction of total lipid content

Total lipid contents (TLC) in all samples were extracted as follows: To a homogenized sample (40 g), 4 ml of 4 M potassium hydroxide solution and 100 ml methanol were added. The mixture was refluxed for two hours. The saponified material was then transferred to a separating funnel and extracted with 25 ml n-pentane. The extract was finally dried and the solvent separated at 50°C to a constant weight

(Abul-Ela, 2004). Concentration of TLC was expressed in μgg^{-1} .

Estimation of PAHs in the samples extracts

All the studied samples were analyzed using high performance liquid chromatography (HPLC) for PAHs detection. Apparatus: Waters HPLC 600, controller 600, Autosampler 717 plus, Dual Absorbance Detector 2487, attached to computerized system with Millennium 32 software. Conditions for operation: Sample: $1\mu\text{l}$. Column: SUPELCOSIL LC-PAHs, 15 cm, 4.6 mm ID, 5 μm particles. Mobile phases: acetonitrile: water 50:50 for 5 min changed gradually to 100% acetonitrile in the next 25 min. Flow rate: 0–2 min, 0.2 ml/min, 2–45 min, 1.0 ml/min. Detector: UV, 254 nm. Standard used: naphthalene (Nap), acetanaphthylene (A), acetanaphthene (Ace), fluoranthene (F), phenanthrene (Phe), anthracene (Ant), fluorene (Flu), pyrene (Pyr), benzo[a]anthracene (BaA), chrysene (Chr), benzo[b]fluoranthene (BbF), benzo[k]fluoranthene (BkF), benzo[a]pyrene (BaP), dibenzo[a,h]anthracene (DahA), benzo[g,h,i]pyrene (BP) and indino[1,2,3-cd]pyrene (IP).

Calculations

Total lipid content (TLC) and PAHs concentrations in 10 samples from each group were calculated and anovated and expressed as mean \pm SD (significance was considered when $p>0.05$); from which the sum of the 16 PAHs concentrations ($\Sigma 16\text{PAH}$), percentage of total PAHs concentrations in relation to the total lipid content (%), in addition to the sum of 6 light

PAHs (≤ 3 rings) concentrations ($\Sigma 6\text{LPAH}$) and the sum of 10 heavy PAHs (≥ 4 rings) concentrations ($\Sigma 10\text{HPAH}$) with their percentages and ring ratios were calculated. Values obtained were expressed in μgg^{-1} . Ring ratios were obtained from the total of each di-, tri-, tetra-, penta- and hexa-aromatics concentrations and were expressed as $\Sigma\text{di-} : \Sigma\text{tri-} : \Sigma\text{tetra-} : \Sigma\text{penta-} : \Sigma\text{hexa-aromatics}$.

Histopathological studies

At each interval, 10 snails were dissected and mantle and gill filaments were removed and fixed in Bouin's solution, washed and restored in 70% alcohol. Tissues were dehydrated in descending grades of alcohol, cleared in xylene and embedded in paraffin. 5 μm paraffin serial sections were cut and routinely stained with haematoxylin and eosin stains, examined on Olympus Microscope and photographed.

RESULTS

Estimation of PAHs burden in experimented *L. carinatus* (Tables 1, 2 and Figures 1-6)

The LC_{50} of crude oil for *L. carinatus* was 700 ppm. HPLC chromatograms of the standard reference of the investigated PAHs, the control samples and treated snails for 24 hrs, 15 days and 30 days postexposure are shown in Figure 1. The concentrations of the 16 PAHs are shown in Table I. TLC, $\Sigma 16\text{PAH}$, $\Sigma 6\text{LPAH}$ and $\Sigma 10\text{HPAH}$ with their percentages and ring ratios were obtained and shown in Table II.

Table I: Distribution and concentrations (in μgg^{-1}) of different PAHs in control and treated snails at 24 hrs, 15 days and 30 days intervals. Nap, naphthalene; A, acetanaphthylene; Ace, acetanaphthene; F, fluoranthene; Phe, phenanthrene; Ant, anthracene; Flu, fluorine; Pyr, pyrene; BaA, benzo[a]anthracene; Chr, chrysene; BbF, benzo[b]fluoranthene; BkF, benzo[k]fluoranthene; BaP, benzo[a]pyrene; DahA, dibenzo[a,h]anthracene; BP benzo[g,h,i]pyrene; IP, indino[1,2,3-cd]pyrene. N resembles Nil

Sample	Nap	A	Ace	F	Phe	Ant	Flue	Pyr	BaA	Chr	BbF	BkF	BaP	DahA	BP	IP
Control	N	N	N	N	N	N	N	N	N	N	N	N	N	N	N	N
24 hrs	N	N	N	N	N	N	N	N	N	N	3.54	N	N	4.41	N	0.3
15 days	N	N	N	N	1.7	1.1	2.09	10.5	9.28	2.29	1.16	N	N	48.87	N	N
30 days	N	N	N	N	N	N	N	N	N	N	N	N	N	3.76	N	1.2

Tables I-II and Figures 1-6 revealed the presence of only Phe, Ant, Flu, Pyr, BaA, Chr, BbF, DahA and IP out of the estimated 16 PAHs (Table I, Figures 1, 5). A transient progressive elevation of TLC from the control with time by

34.97% at 24 hrs and 855.7 % at 15 days, followed by 23.22% regression at 30 days of exposure (Table II, Figure 2a). PAHs content (% of $\Sigma 16\text{PAH}$) were directly proportional to the total lipid content at all time periods (Table II,

Figures. 3a, b) and all fluctuated around 0.5% of TLC (Figure 2b).PAHs accumulation ($\Sigma 16\text{PAH}$) in treated *L. carinatus* was pronounced at 24 hrs with an elevation in 15 days-exposed snails followed by PAHs content decline at 30 days (Table II, Figures 2b, 3a, b).Light PAHs were observed at only 15 days of exposure, and were

recorded at relatively low concentrations in addition to tetra- and penta-aromatics, while only penta-aromatics were obtained at 24 hrs-treated snails and penta- and hexa-aromatics were obtained at 30 days-treated snails (Table II, Figures 4-6).

Table II: Total lipid contents (TLC, in $\mu\text{g g}^{-1}$) and sum of 16 PAHs concentrations ($\Sigma 16\text{PAH}$) in addition to the sum of 6 light PAHs (≤ 3 rings) concentrations ($\Sigma 6\text{LPAH}$), the sum of 10 heavy PAHs (≥ 4 rings) concentrations ($\Sigma 10\text{HPAH}$) with their percentages and ring ratios for the control and treated samples at 24 hrs, 15 days and 30 days intervals. Concentrations are in $\mu\text{g g}^{-1}$.

Sample	TLC	$\Sigma 16\text{PAH}$	%	$\Sigma 6\text{LPAH}$	%	$\Sigma 10\text{HPAH}$	%	Ring ratio
Control	1490	0	0	0	0	0	0	0:0:0:0:0
24 hrs	2011	8.25	0.41	0	0	8.25	100	0:0:0:8:0
15 days	14240	77.02	0.54	2.83	3.67	74.19	9633	0:3:24:50:0
30 days	1144	5	0.44	0	0	5	100	0:0:0:4:1

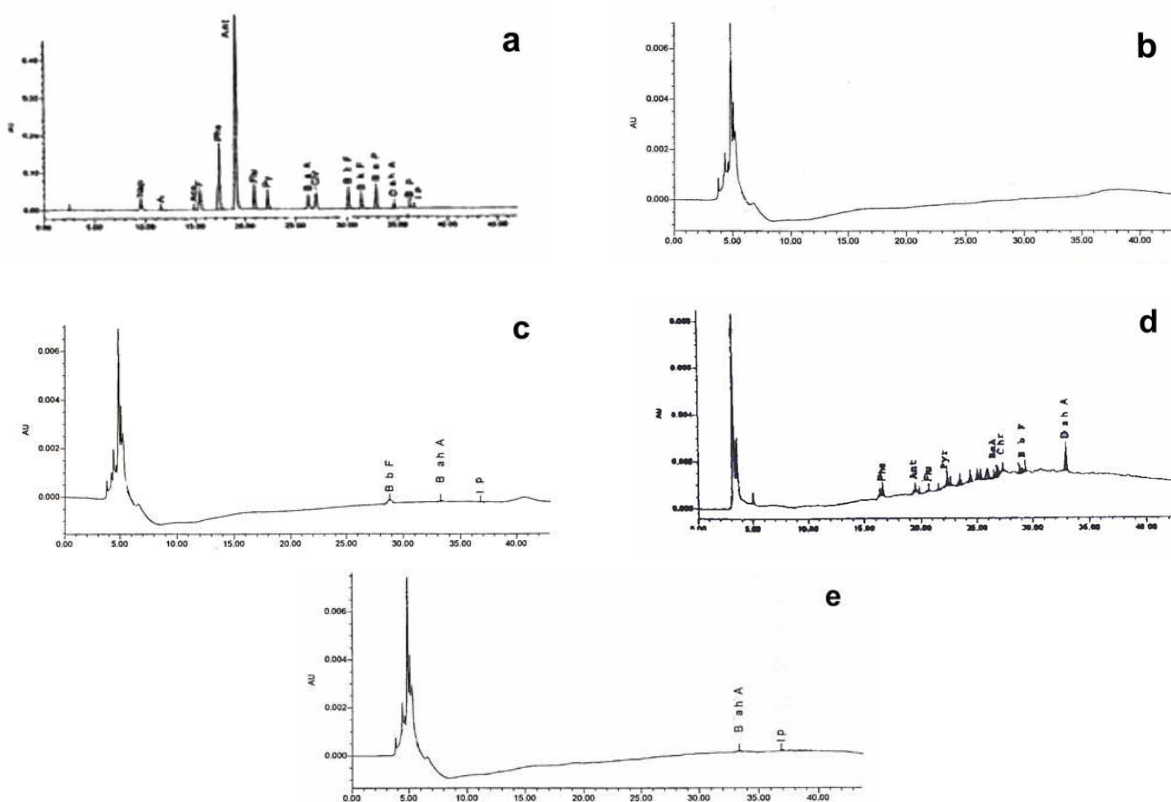


Figure 1: HPLC chromatograms of: a, standard PAHs reference; b, control snails, c, 24 hours treated snails, d, 15 days treated snails, e, 30 days treated snails. Nap, naphthalene; A, acetanaphthylene; Ace, acetanaphthene; F, fluoranthene; Phe, phenanthrene; Ant, anthracene; Flu, fluorine; Pyr, pyrene; BaA, benzo[a]anthracene; Chr, chrysene; BbF, benzo[b]fluoranthene; BkF, benzo[k]fluoranthene; BaP, benzo[a]pyrene; DahA, dibenzo[a,h]anthracene; BP benzo[g,h,i]pyrene; IP, indino[1,2,3-cd]pyrene.

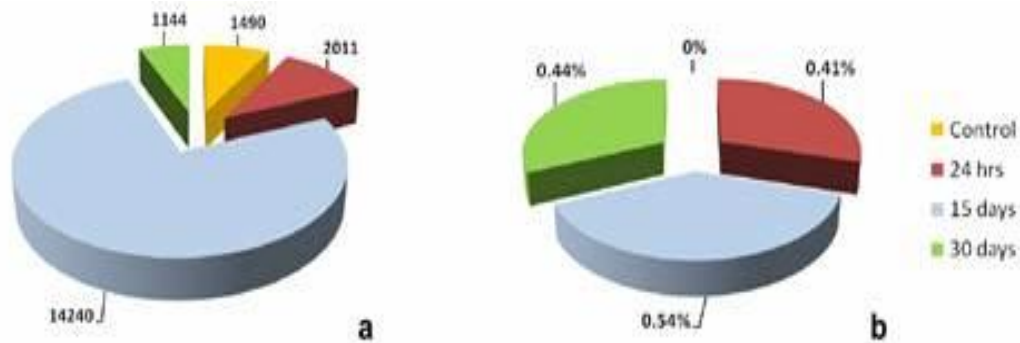


Figure 2: a, concentrations (in $\mu\text{g g}^{-1}$) of total lipid contents (TLC) and b, percentages of $\Sigma 16\text{PAHs}$ in the control and treated samples.

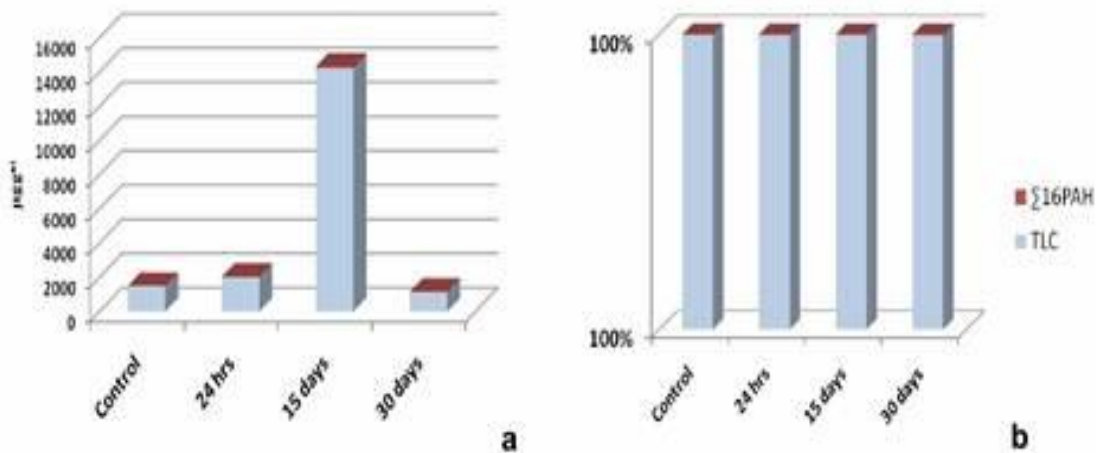


Figure 3: a, concentrations (in $\mu\text{g g}^{-1}$) and b, percentages of total lipid content (TLC) and $\Sigma 16\text{PAHs}$ in the control and treated samples.

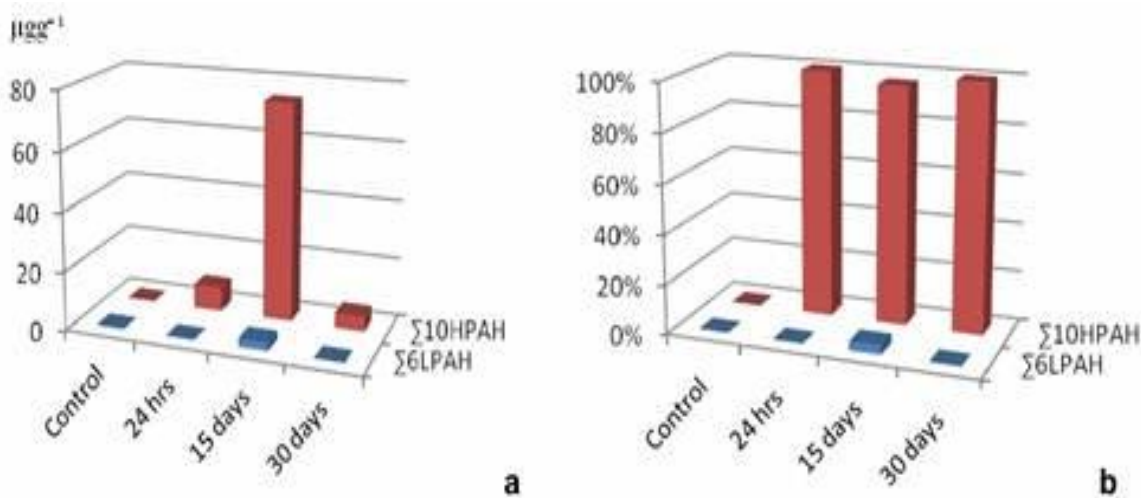


Figure 4: a, concentrations (in $\mu\text{g g}^{-1}$) and b, percentages of $\Sigma 6\text{LPAH}$ and $\Sigma 10\text{HPAH}$ in the control and treated samples.

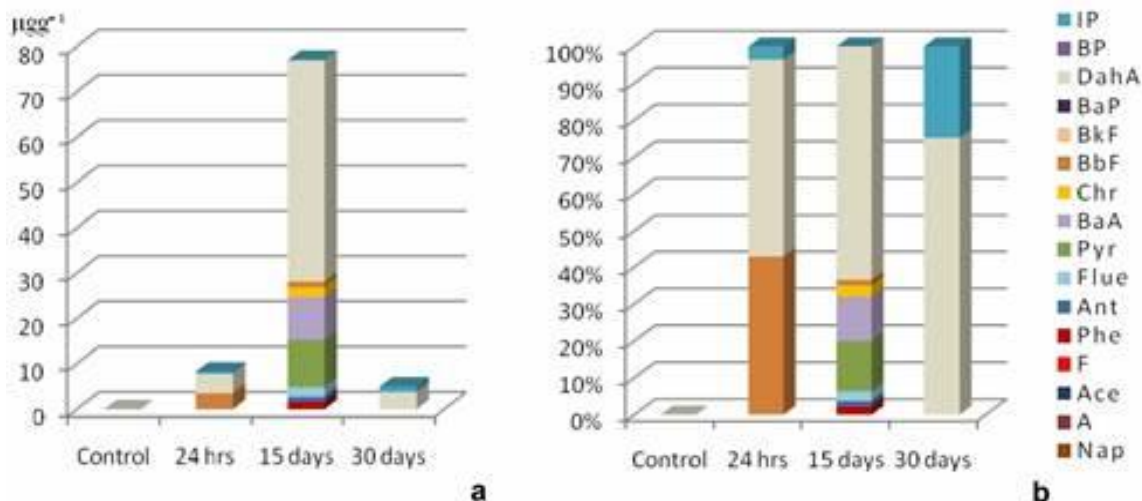


Figure 5: a, concentrations (in $\mu\text{g g}^{-1}$) and b, percentages of various PAHs in the control and treated samples.

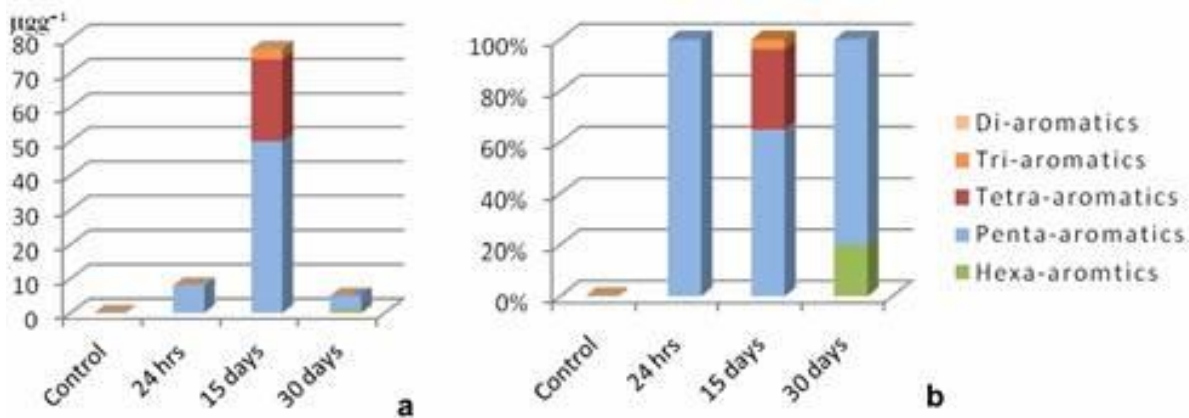


Figure 6: a, concentrations (in $\mu\text{g g}^{-1}$) and b, percentages of ring ratios of the evaluated PAHs in the control and treated samples.

Histological structure of control snails (Figure 7)

Examination of the mantle of *L. carinatus* revealed the presence of surface epithelia inverted by mucous cells followed by layers of prickle-shaped granulosa cells resting on abasement membrane. Large mucous cells were seen originating in this layer and drawn upward to the surface epithelia. Just beneath this layer was a collagenous muscle layer, the tunica externa, followed by a thick layer of smooth muscles, mucosa muscularis, the vasculized submucosa, which was composed of loose connective tissue and defused by sinusoids, adipose cells and lymphocytes, and lastly the tunica interna. Gill filaments were composed of columnar epithelia with well developed simple ciliary structures at the distal

end resembling frontal, laterofrontal and lateral cilia, followed by pillar cells resting on abasement membrane and inverted by mucous cells. The sinusoids were lined with a thin collagenous muscle layer and filled with the haemal fluid and lymphocytes.

Examination of treated snails at 24 hrs postexposure (Figure 8)

Microscopic examination of the mantle and gill filaments revealed epithelial hypertrophy, hyperplasia, epithelial lifting, lamellar fusions, telangiectasia, inflammation, lymphocytic congestion, shrunken and undulating cilia and mucous cell hyperplasia. Moreover, the pallial epithelia showed proliferation of dense bodies in their cytoplasm, in addition to extensive mucous secretions. Degeneration, inflammation,

necrosis, extensive lymphocytic infiltration, edema and eosinophilic reactions in tunica

externa, mucosa, submucosa and sinusoids were also observed.

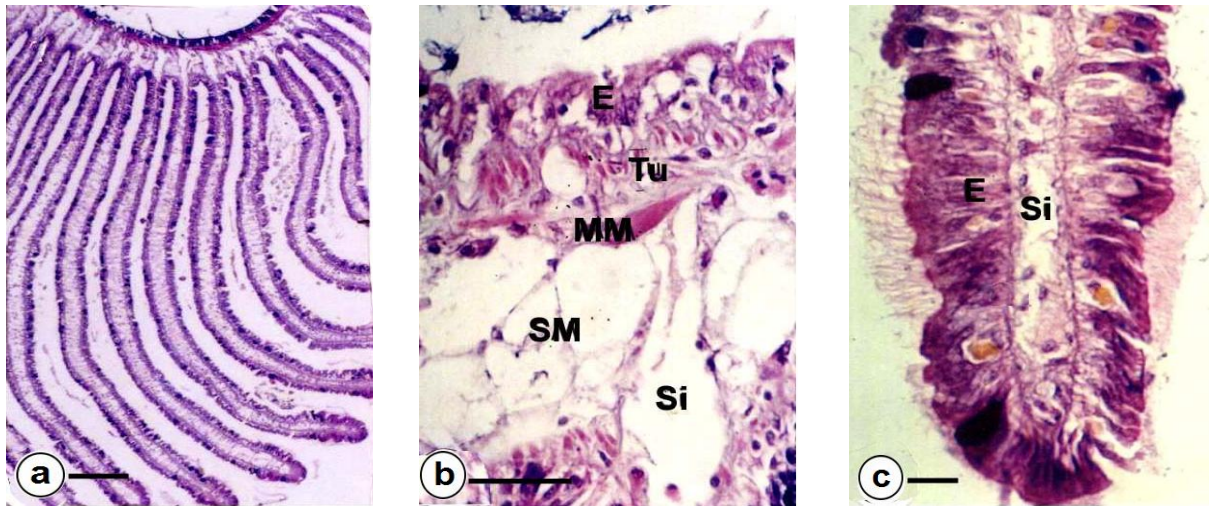


Figure 7: Photomicrographs of the mantle and gill filaments of control *L. carinatus*. a) Showing the general construction of mantle and gill filaments. b) L.S. in the mantle showing epithelial layer followed by tunica externa, mucosa muscularis and submucosa inverted by sinusoids. c) L.S. in the distal part of a gill filament. It composed of epithelial layer inverted by mucous cells and a sinusoid that lined by collagenous layer and containing lymphocytes. Note the frontal, laterofrontal and lateral cilia that formed by epithelial cells. C, cilia; E, epithelial layer; MM, muscular mucosa; Si, sinusoid; SM, submucosa; Tu, tunica externa; Scale bar a) = 200 μ m; b,c) = 20 μ m.

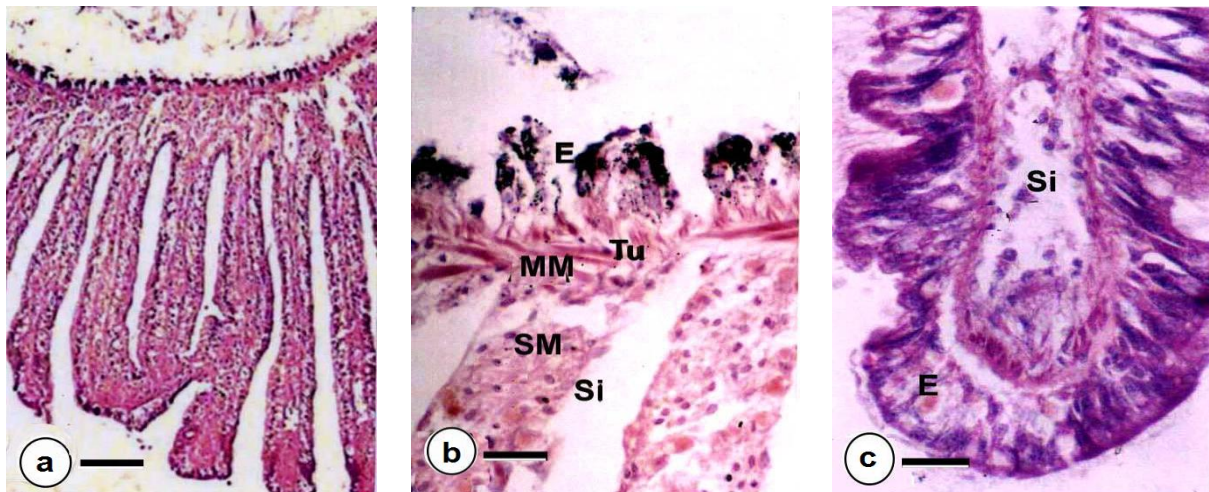


Figure 8: Photomicrographs of the mantle and gill filaments of 24 hrs-treated *L. carinatus*. a) Showing the sinusoid congestion, dilation and lamellar fusion of the gill filaments. b) L.S. in the mantle manifesting proliferative changes. Note the hypertrophy, hyperplasia, destruction, degeneration, pigment deposition, lifting and extensive mucous formation in the epithelial cells. Note also the excessive stainability in tunica externa and mucosa muscularis, lymphocytic infiltration, edema and degeneration in the submucosa and sinusoids dilation. c) L.S. in the distal part of a gill filament showing inflammation with shrunken and undulating cilia in the surface epithelium and dilated sinusoid. C, cilia; E, epithelial layer; MM, muscular mucosa; Si, sinusoid; SM, submucosa; Tu, tunica externa; Scale bar a) = 200 μ m; b,c) = 20 μ m.

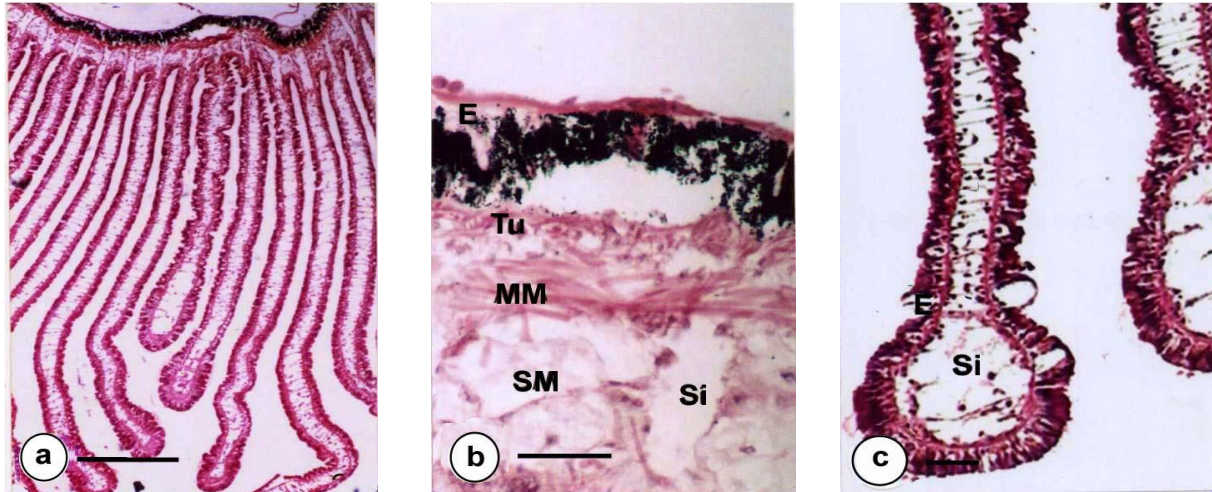


Figure 9: Photomicrographs of the mantle and gill filaments of 15 days-treated *L. carinatus*. a) L.S. showing the reduction of the mantle layers thickness. Note the lamellar shrinkage and curling with decongested and dilated sinusoids. b) L.S. in the mantle manifesting proliferative changes. Note the pigment deposition, lifting, mucous malformation and the filamentous coat in the surface epithelium. Note also the lymphocyte reduction, edema and degeneration in the submucosa and sinusoids dilation. c) L.S. in the distal part of a gill filament showing telangiectasia with bulbous ends, hypertrophy, hyperplasia, metaplastic desquamation, disintegration, necrosis, mucous malformation, shrinking and loss of cilia. Note also the thickening of sinusoid wall and deviation of lymphocytes. E, epithelial layer; MM, muscular mucosa; Si, sinusoid; SM, submucosa; Tu, tunica externa; Scale bar a) = 200 μ m; b,c) = 20 μ m.

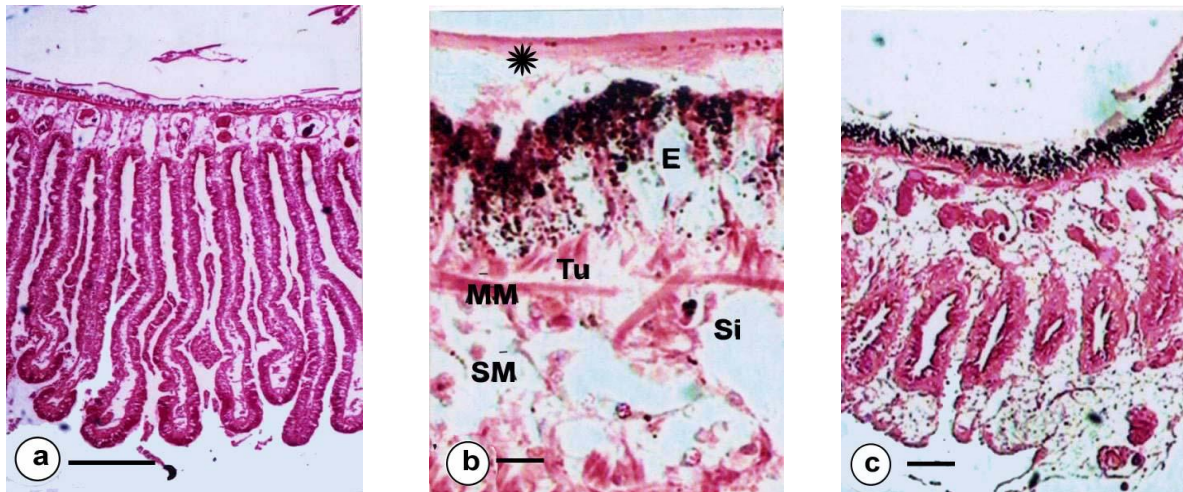


Figure 10: Photomicrographs of the mantle and gill filaments of 30 days-treated *L. carinatus*. a) L.S. in mantle and gill filaments showing general reduction in size caliber of the mantle, curling, forked and shortening of gill filaments with vesiculated fibrous conglomerates in the sinusoids. b) L.S. in the mantle showing reduced epithelial cells being distended with pigments in addition to epithelial lifting and proliferation of filamentous coat (asterisk). Reduction in size, necrosis, edema and scarce lymphocytic infiltration in tunica externa, mucosa muscularis and submucosa and further dilations in the sinusoids are also prominent. c) L.S. in gill filaments manifesting filamentous fusion composed of collagenous fibers and adipose tissue E, epithelial layer; MM, muscular mucosa; Si, sinusoid; SM, submucosa; Tu, tunica externa; Scale bar a) = 200 μ m; b,c) = 20 μ m.

Examination of treated snails at 15 days postexposure (Figure 9)

The pallial epithelia showed extensive dense bodies and lateral, ill-defined or diminished nuclei. They appeared coated with filamentous material with a marked reduction in mucous formation. Degenerative and necrotic changes were evidently observed in tunica externa, mucosamuscularis and submucosa that showed further reduction in thickness with obvious edema and less lymphocytic infiltration. The gill filaments appeared shrunken and curled with broader and dilated bulbous ends. Epithelial vacuolation, hypertrophy, hyperplasia, epithelial disintegration, lifting, metaplastic desquamation, loss and shrunken cilia, different degrees of cytoplasmic and karyotic necrosis, sinusoid telangiectasia with lymphocytic deviation and fusions being filled with fibrous matrix were readily observed. Distinct malformed hypertrophied arrested mucous cells restricted primarily at the pillar layer were also detected.

Examination of treated snails at 30 days postexposure (Figure 10)

Extensive necrotic changes were the prominent feature of the tissue in all parts. Pallial epithelia showed a dense coat of filamentous material and further reduction in dense bodies and mucous. The sinusoids appeared much dilated and exhibited vesiculated fibrous conglomerates. Gill filaments appeared curled and reduced in general caliber with an evident deposition of collagen in sinusoids were detected in a wide spectrum. The forked and fused filaments were composed of fibrous and adipose connective tissues.

DISCUSSION

In the present investigation, the results showed that TLC during the treatment showed a marked fluctuation with time than control (34.97%, 855.7% and -23.22% at 24 hrs, 15 days and 30 days post exposure respectively. These findings agreed with Smolders *et al.* (2002) who reported changes in lipid content in mussels according to period of exposure and level of contamination. Total PAHs content percentages seem to be directly proportional to TLC at all the time periods and all were being fluctuated around 0.5%. There may be accordingly a possible direct proportional relationship between TLC of the animal and

bioaccumulation of PAHs, which in turn seems to be time related. Such relationship is quite reasonable since PAHs are fat soluble compounds and tend to accumulate primarily in lipids. In this investigation, PAHs accumulation in the treated snails was pronounced at 24 hrs of exposure with maximal elevation peak at 15 days, including tri-, tetra- and penta-aromatics, and then declined on the day 30th of exposure including only penta- and hexa-aromatics. It is suggested that accumulation of these contaminants involves transformation during metabolism which regulates the fate of their accumulation in the tissue. McDonnell and Dang (2013) and Dalzochio *et al.* (2016) stated that cytochrome P450s are monooxygenases responsible by a set of functions for controlling homeostasis, including the metabolism of xenobiotics. In phase I, the first stage of detoxification of hydrocarbons implicates enzymatic transformation of a chemically modifying lipid soluble toxin into water-soluble toxin (Lardone *et al.*, 2010). Phase II antioxidant enzymes (as catalase, CAT and glutathione-S-transferase, GST) are involved in the second stage of the detoxification process modify phase I products into more water-soluble and less toxic forms (Azevedo *et al.*, 2013; Hassan *et al.*, 2015).

The histopathological alterations encountered in gill filaments in response to petroleum exposure at 24 hrs resemble typical manifestations of acute toxicity. These manifestations were implied in contour of reversible cellular defensive behaviors to meet extra defensive demands to overcome the pollution. Such cellular behaviors include adaptation (epithelial hypertrophy, hyperplasia, desquamation, lifting and lamellar fusions proliferation of microvilli and mucous oversecretions), inflammation (lymphocytic infiltration, telangiectasia, edema, eosinophilic cytoplasm and lamellar congestion) and degeneration (necrosis and collagen deposition). Lesions encountered at 15 days post exposure can be pathologically explained in the frame of reversible injury due to persistence of the stressor. These include deposition of microfilaments, collagen, edema, less lymphocytic infiltration and malformed hypertrophied arrested mucous cells. Further linear decline in cellular numbers and necrotic changes encountered in the samples at 30 days post exposure seem to be chronic irreversible changes and depend on continued exposure

toxicants and on the concentration administered. The histopathological changes encountered in gill filaments in response to petroleum exposure amongst various intervals in the present investigation are typical lesions similar to alterations in gills in invertebrates studied by several authors for a wide range of toxicants. Sublethal concentrations of other pollutants such as copper (5, 10, 25, 50, and 75 $\mu\text{gCu}^{2+}\text{L}^{-1}$) and lithium (50, 100, 200, 1000 and 5000 $\mu\text{gLi}^{+}\text{L}^{-1}$) were found to induce collective lesions of identical histopathological alterations in the gill of ramshorn snail, *Marisa cornuarietis*, including irregularly shaped cilia and changes in the amount of mucus (Sawasdee *et al.*, 2011). Chakraborty *et al.* (2010) investigated histopathological damages in the gill of the Indian bivalve *L. marginalis* exposed to sublethal concentrations of sodium arsenite for 30 days leading eventually to tissue dysfunction. Additional Mollusks tissues showed similar alterations in response to various pollutants. *M. cornuarietis* exposed to copper and lithium (Sawasdee *et al.*, 2011) showed changes in epithelial and mucous cells of the epidermis

In the present work, the dramatic linear proliferation in necrotic changes may be due to cellular oxidation in response to toxicants. Sandrini-Neto *et al.* (2016) recorded oxidative damage and antioxidant responses concurrently associated with changes in oxidative enzymes as superoxide dismutase (SOD), GST and lipid peroxidation (LPO) levels in the bivalve *Anomalocardia brasiliensis*, the gastropod *Neritina virginea* and the polychaete *Laeonereis culveri*, in response to oil spills and diesel. Liu *et al.* (2014) in their study on gills and digestive gland of clams (*Ruditapes philippinarum*) exposed to 0.03, 0.3 and 3 $\mu\text{g/L}$ B[a]P for 21 days assayed the changes in B[a]P metabolite contents, activities of aryl hydrocarbon hydroxylase (AHH), 7-ethoxyresorufin O-deethylase (EROD), epoxide hydrolase (EH), dihydrodiol dehydrogenase (DD), GST, sulfotransferase (SULT) and uridinediphosphate glucuronyl transferase (UGT) which correlated with oxidation and B[a]P bioaccumulation. These oxidative alterations may affect the permeability and function of the cell membrane and other organelles and eventually the cell function.

In this study, the palial epithelia showed enhanced extensive dense bodies which may refer to transformation of lysosomes into lipofusins in response to crude oil exposure. Au (2004) documented that lipopigments tend to accumulate in the lysosomal compartment as

residual bodies, which may be related to disturbance of lysosomal system functioning and was recommended as a biomarker in the monitoring programs.

In this study, enhanced proliferation of some structural compartments as the deposition of collagen and lipid was recorded which seems to be cumulative with time. This is likely to be in part a broad response to toxicants, however, it is not known whether it play a role in storage or detoxification of the pollutant. Similar deposition of such materials was recorded in previous works. Silva *et al.* (2017) indicated changes in lipid profile in the marine prosobranch *Gibbulaum bilicalis* in response to metal exposure by nickel, cadmium and mercury for 168 hrs and suggested that such a biomarker may correlated in some extent to homeoviscous adaptation and immune response of the snail.

In conclusion, the potential value of the freshwater prosobranch *L. carinatus* as a biological monitor to crude oil pollution is investigated in PAHs bioaccumulation and histopathological changes. Such changes are repeatedly included in monitoring programs and are proposed to affect the respiratory function of the gills and subsequently threaten the animal life and its persistence. Thus, *L. carinatus* suggested to be an effective biological monitor for crude oil pollution in freshwater.

REFERENCES

- ABUL-ELA, M.A.S., 2004. Studies on oil pollutants in some important Egyptian marine environments. *M.Sc. Thesis, Ain Shams University, Egypt.*
- ANDLEEB, S., 2014. A comprehensive review on chromium: toxicities and detoxification. *Punjab Univ. J. Zool.*, **29**: 41-62.
- AU, D.W.T., 2004. The application of histocytopathological biomarkers in marine pollution monitoring: a review. *Mar. Pollut. Bull.*, **48**: 817-834.
- AZEVEDO, J.S., BRAGA, E.S., ASSIS, H.C.E. AND RIBEIRO, C.A.O., 2013. Biochemical changes in the liver and gill of *Cathoropsspaxii* collected seasonally in two Brazilian estuaries under varying influences of anthropogenic activities. *Ecotoxicol. Environ. Safety*, **96**: 220-230.
- BAKER, L.F., CIBOROWSKI, J.J.H. AND MACKINNON, M.D., 2012. Petroleum

- coke and soft tailings sediment in constructed wetlands may contribute to the uptake of trace metals by algae and aquatic invertebrates. *Sci. Total. Environ.*, **414**: 177-186.
- BEJARANO, A.C. AND MICHEL, J., 2016. Oil spills and their impacts on sand beach invertebrate communities: A literature review. *Environ. Poll.*, **218**: 709-722.
- CAI, Y., PAN, L. AND MIAO, L., 2016. In vitro study of the effect of metabolism enzymes on benzo(a)pyrene-induced DNA damage in the scallop *Chlamys farreri*. *Environ. Toxicol. Pharmacol.*, **42**: 92-98.
- CHAKRABORTY, S., RAY, M. AND RAY, S., 2010. Toxicity of sodium arsenite in the gill of an economically important mollusc of India. *Fish Shellfish Immunol.*, **29**: 136-148.
- DALZUCHIO, T., RODRIGUES, G.Z.P., PETRY, I.E., GEHLEN, G. AND DA SILVA, L.B., 2016. The use of biomarkers to assess the health of aquatic ecosystems in Brazil: a review. *Int. Aquat. Res.*, **8**: 283-298.
- GROSELL, M. AND BRIX, K.V., 2009. High net calcium uptake explains the hypersensitivity of the freshwater pulmonate snail, *Lymnaea stagnalis*, to chronic lead exposure. *Aquat. Toxicol.*, **91**: 302-311.
- HASSAN, I., JABIR, N.R., AHMAD, S., SHAH, A. AND TABREZ, S., 2015. Certain phase I and II enzymes as toxicity biomarker: an overview. *Water Air Soil Pollut.*, **226**: 153.
- JEMEC, A., DROBNE, D., TISLER, T. AND SEPCIĆ, K., 2010. Biochemical biomarkers in environmental studies-lessons learnt from enzymes catalase, glutathione S-transferase and cholinesterase in two crustacean species. *Environ. Sci. Pollut. Res. Int.*, **17**(3): 571-581.
- LARDONE, M.C., CASTILLO, P., VALDEVENITO, R., EBENSPERGER, M., RONCO, A.M., POMMER, R., PIOTTANTE, A. AND CASTRO, A., 2010. P450-aromatase activity and expression in human testicular tissues with severe spermatogenic failure. *Int. J. Androl.*, **33**: 650-660.
- LITCHFIELD, J.T.Jr. AND WILCOXON, F., 1949. A simplified method of evaluating dose-effect experiments. *J. Pharmacol. Exp. Ther.*, **96**: 99-113.
- LIU, D., PAN, L.I.Z., CAI, Y. AND MIAO, J., 2014. Metabolites analysis, metabolic enzyme activities and bioaccumulation in the clam *Ruditapes philippinarum* exposed to benzo[a]pyrene. *Ecotoxicol. Environ. Safety*, **107**: 251-259.
- MCDONNELL, A.M. AND DANG, C.H., 2013. Basic review of the cytochrome P450 system. *J. Adv. Pract. Oncol.*, **4**: 263-268.
- OSTERAUER, R., HAUS, N., SURES, B. AND KÖHLER, H.-R., 2009. Uptake of platinum by zebrafish (*Danio rerio*) and ramshorn snail (*Marisa cornuarietis*) and resulting effects on early embryogenesis. *Chemosphere*, **77**: 975-982.
- SANDRINI-NETO, L., PEREIRA, L., CÉSAR, C., MARTINS, C.C., SILVA DE ASSIS, H.C., CAMUS, L. AND LANA, P.L., 2016. Antioxidant responses in estuarine invertebrates exposed to repeated oil spills: Effects of frequency and dosage in a field manipulative experiment. *Aquat. Toxicol.*, **177**: 237-249.
- SANNI, S., LYNG, E., PAMPANIN, D.M. AND SMIT, M.D.G., 2016. I. Species sensitivity distributions based on biomarkers and whole organism responses for integrated impact and risk assessment criteria. *Mar. Environ. Res.*, (In Press)
- SARKARA, A., BHAGAT, J. AND SARKER, S., 2014. Evaluation of impairment of DNA in marine gastropod, *Morula granulata* as a biomarker of marine pollution. *Ecotoxicol. Environ. Safety*, **106**: 253-261.
- SARKARA, A., DIPAK, I., GAITONDEB, C.S., SARKARA, I.A., VASHISTHAA, D., D'SILVAA, C. AND DALALA, S.G. 2008. Evaluation of impairment of DNA integrity in marine gastropods (*Croniacon tracta*) as a biomarker of genotoxic contaminants in coastal water around Goa, West coast of India. *Ecotoxicol. Environ. Safety*, **71**: 473-482.
- SAWASDEE, B., KÖHLER, H.R. AND TRIEBSKORN, R., 2011. Histopathological effects of copper and lithium in the ramshorn snail, *Marisa cornuarietis* (Gastropoda,

- Prosobranchia). *Chemosphere*, **85**: 1033-1039.
- SILVA, C.L., SIMÕES, T., NOVAIS, S.C., PIMPAREL, I., GRANADA, L., SOARES, A.M.V.M., BARATA, C. AND LEMOS, M.F.L., 2017. Fatty acid profile of the sea snail *Gibbulaum bilicalis* as a biomarker for coastal metal pollution. *Sci. Total Environ.*, In Press.
- SMOLDERS, R., BERVOETS, L. AND BLUUST, R., 2002. Transplanted zebra mussels (*Dreissena polymorpha*) as active biomonitors in an effluent dominated river. *Environ. Toxicol. Chem.*, **21**: 1889-1896.
- TANIA, Y.N.G.-T., PAIS, N.M. AND WOOD, C.M., 2011. Mechanisms of waterborne Cu toxicity to the pond snail *Lymnaeostagnalis*: Physiology and Cu bioavailability. *Ecotoxicol. Environ. Safety*, **74**: 1471-1479.
- WHO, 1993. Environmental Health Criteria 155: Biomarkers and Risk Assessment: Concepts and Principles.